

University of Montana

## ScholarWorks at University of Montana

---

Numerical Terradynamic Simulation Group  
Publications

Numerical Terradynamic Simulation Group

---

12-2014

### Asynchronous Amazon forest canopy phenology indicates adaptation to both water and light availability

Matthew O. Jones

John S. Kimball

*University of Montana - Missoula*

Ramakrishna R. Nemani

Follow this and additional works at: [https://scholarworks.umt.edu/ntsg\\_pubs](https://scholarworks.umt.edu/ntsg_pubs)

**Let us know how access to this document benefits you.**

---

#### Recommended Citation

Jones, M. O., Kimball J. S., and Nemani R. R. (2014). Asynchronous Amazon forest canopy phenology indicates adaptation to both water and light availability. *Environmental Research Letters*, 9(12): 10 pp. doi: 10.1088/1748-9326/9/12/124021

This Article is brought to you for free and open access by the Numerical Terradynamic Simulation Group at ScholarWorks at University of Montana. It has been accepted for inclusion in Numerical Terradynamic Simulation Group Publications by an authorized administrator of ScholarWorks at University of Montana. For more information, please contact [scholarworks@mso.umt.edu](mailto:scholarworks@mso.umt.edu).

# Asynchronous Amazon forest canopy phenology indicates adaptation to both water and light availability

Matthew O Jones<sup>1,3</sup>, John S Kimball<sup>1</sup> and Ramakrishna R Nemani<sup>2</sup>

<sup>1</sup>Flathead Lake Biological Station/Numerical Terradynamic Simulation Group, University of Montana, Missoula, MT, USA

<sup>2</sup>NASA Advanced Supercomputing Division, NASA Ames Research Center, Moffett Field, CA, USA

E-mail: [matt.jones@ntsug.umt.edu](mailto:matt.jones@ntsug.umt.edu)


Received 22 September 2014, revised 21 November 2014

Accepted for publication 25 November 2014

Published 18 December 2014

## Abstract

Amazon forests represent nearly half of all tropical vegetation biomass and, through photosynthesis and respiration, annually process more than twice the amount of estimated carbon (CO<sub>2</sub>) from fossil fuel emissions. Yet the seasonality of Amazon canopy cover, and the extent to which seasonal fluctuations in water availability and photosynthetically available radiation influence these processes, is still poorly understood. Implementing six remotely sensed data sets spanning nine years (2003–2011), with reported field and flux tower data, we show that southern equatorial Amazon forests exhibit a distinctive seasonal signal. Seasonal timing of water availability, canopy biomass growth and net leaf flush are asynchronous in regions with short dry seasons and become more synchronous across a west-to-east longitudinal moisture gradient of increasing dry season. Forest cover is responsive to seasonal disparities in both water and solar radiation availability, temporally adjusting net leaf flush to maximize use of these generally abundant resources, while reducing drought susceptibility. An accurate characterization of this asynchronous behavior allows for improved understanding of canopy phenology across contiguous tropical forests and their sensitivity to climate variability and drought.

 Online supplementary data available from [stacks.iop.org/ERL/9/124021/mmedia](http://stacks.iop.org/ERL/9/124021/mmedia)

Keywords: vegetation optical depth, AMSR-E, amazon, phenology, seasonality, tropical forests

## 1. Introduction

Amazon forests are a major component of the global carbon (C) cycle, processing ~18 Pg C annually through photosynthetic uptake and respiration of atmospheric CO<sub>2</sub> (Christensen *et al* 2007), and representing nearly half of all tropical vegetation biomass (Saatchi *et al* 2011). Projected drying

from climate change (Salazar *et al* 2007, Cox *et al* 2008) may alter the regional C balance and the critical role of these forests in the global C cycle (Cox *et al* 2013). For example, widespread drought in 2005 and 2010 and subsequent effects on forest mortality (Phillips *et al* 2009, Lewis *et al* 2011) and canopy greenness (Xu *et al* 2011) may become more typical future scenarios (Li *et al* 2008, Lee *et al* 2011). Predicting long-term vegetation responses to a changing climate is complex (Cox *et al* 2013), but understanding how Amazon forest canopy phenology has adapted to seasonal changes in water and light availability may provide insight into forest behavior under future climate conditions (Malhi *et al* 2009).

The climatic constraints of water and light availability on forest growth in the Amazon are small when compared to more temperate systems with clear active and dormant

<sup>3</sup> University of Montana—NTSG, DHC 021, 32 Campus Missoula, MT 59812, USA.



Content from this work may be used under the terms of the Creative Commons Attribution 3.0 licence. Any further distribution of this work must maintain attribution to the author(s) and the title of the work, journal citation and DOI.

seasons, yet the majority of the region experiences peaks in solar irradiance out of phase with precipitation due to cloud cover seasonality (Restrepo-Coupe *et al* 2013). The extent to which seasonal fluctuations of these constraints control Amazon canopy phenology is still poorly understood. This is due in part to the wide species diversity and variety of phenological patterns in tropical forests where leaf flush and senescence are continuous processes. Satellite remote sensing however provides a spatially integrated measure of canopy scale net leaf flush (i.e. the majority of species exhibiting new leaf growth). Satellite and field observations have demonstrated that net leaf flush is often asynchronous with peaks in water availability, woody growth, canopy greenness, photosynthetic capacity ( $P_c$ ), and gross ecosystem productivity (GEP) (Myneni *et al* 2007, Samanta *et al* 2012, Lee *et al* 2013, Restrepo-Coupe *et al* 2013, Rowland *et al* 2014), which has further confounded an integrated understanding of light and water availability effects on Amazon canopy phenology.

Reliable satellite optical-infrared remote sensing observations are hindered in the Amazon by persistent clouds, smoke and atmosphere aerosol contamination, and signal saturation over dense broadleaf forests. These measurement difficulties spurred a contrary report claiming Amazon forests display no seasonality in canopy greenness and structure (Morton *et al* 2014), yet the majority of data from in situ to basin wide scales confirm forest canopy seasonality (Saleska *et al* 2003, Asner *et al* 2004, Goulden and Miller 2004, Rice *et al* 2004, Barlow *et al* 2007, Fisher *et al* 2007, Doughty and Goulden 2008, Brando *et al* 2010, Lee *et al* 2013, Parazoo *et al* 2013, Frankenberg *et al* 2014). Also, a relatively long historical satellite record and sophisticated data processing has allowed for identification of Amazon canopy seasonality (Myneni *et al* 2007, Samanta *et al* 2012, Silva *et al* 2013), including observed seasonal changes in canopy biomass from satellite active and passive microwave sensors (Frolking *et al* 2011, Jones *et al* 2011) that are insensitive to solar illumination, cloud and atmospheric effects. Amazon canopies are also vertically and spatially complex, and remote sensing observations over intact forests primarily represent upper canopy conditions. These observations cannot be readily extrapolated to the lower canopy and understory, which may display different phenological processes responsive to a far more variable light regime dependent on canopy architecture. Proper characterization therefore requires the use of multiple satellite measures across a range of frequencies and coupled with ground based observations to measure and compare multiple aspects of Amazon phenology. This coupled strategy builds confidence in satellite retrievals by reducing dependency on any single observation source.

To better characterize Amazon canopy phenology we use six remotely sensed data sets spanning nine years (2003–2011), in context with reported field and flux tower data. This study aims to elucidate Amazon forest canopy phenology and provide a methodology for pixel-wise mapping of the extent to which canopy phenology has adapted to light and/or water availability across a longitudinal moisture gradient. We address the following questions. First, are

canopy net leaf flush and increases in vegetation canopy biomass water content asynchronous across the Amazon? Second, if asynchrony is present, does the degree of asynchrony show a dependence on water availability and photosynthetically active radiation (PAR)?

## 2. Background on tropical phenology modeling and theory

The observed asynchronous behavior of these forests and severe constraints on remote sensing observations has posed a challenge to improving understanding and model predictions of Amazon canopy phenology, primary productivity and vegetation–atmosphere interactions. Early models (e.g. Moorcroft *et al* 2001) implemented a drought-deciduous phenology (leaf abscission occurs when plant available water (PAW) drops below a critical threshold), which failed to represent observed canopy phenology over tropical systems where PAW is often abundant, and leaf growth is synchronous with light availability. Recent terrestrial biosphere and land surface models implemented a satellite derived enhanced vegetation index (EVI) to capture leaf  $P_c$  (Xiao *et al* 2005) and parameters for root water uptake and hydraulic redistribution (Lee and Oliveira 2005, Baker *et al* 2008) to allow for dry season evapotranspiration increases. These models showed improved GEP accuracy against tower observations, but still lacked proper characterization of canopy leafing phenology. To better capture canopy phenology, Kim *et al* (2012) developed a light-controlled phenology sub-model which improved model simulation of seasonal carbon fluxes over a flux tower footprint, and indicated that light-controlled phenology may act as a source of resilience to climate variability.

The light-controlled phenology sub-model (Kim *et al* 2012) supports the theory that in the absence of water deficits tree phenologies have been selected to coincide with peaks in solar irradiance (Wright 1996) and subsequently that tropical forest canopy net leaf flushing is responsive to irradiance seasonality. Seasonal changes in water availability, irradiance and insect activity (e.g. herbivory) are expected to have consistent effects across the majority of tropical forest species (Wright 1996). When water deficits are absent, selection will favor net leaf production during periods of low herbivory and high irradiance. In contrast, when seasonal water deficits are sufficient to detrimentally affect plant cell expansion and growth, trees must produce leaves during periods of adequate water availability. Data compiled from 53 worldwide studies of tropical plant phenology (Schaik *et al* 1993) and an experiment over four evergreen tropical forests (Wright and Schaik 1994) demonstrated that canopy net leaf flushing coincides with seasonal solar maxima. More recently, a study of Amazon tower flux data across multiple years and sites (Restrepo-Coupe *et al* 2013) implemented two leaf-flush models and found a consistent positive correlation between leaf flush and light availability. The work presented here provides further support that leaf growth is responsive to irradiance seasonality in the Amazon, examining this

hypothesis beyond the scale of plot level data and flux tower footprints by incorporating a suite of remote sensing data and taking account of the longitudinal gradient in water versus light availability across the Amazon.

### 3. Methods

#### 3.1. GRACE terrestrial water storage (TWS)

The GRACE mission provides measurements of spatio-temporal changes in Earth's gravity field which can be used to derive changes in TWS, and has been implemented in previous studies over the Amazon (Chen *et al* 2010, Frappart *et al* 2013, Thomas and Reager 2014). We use the GRACE GRCTellus Monthly Mass Grids-Land product (Swenson and Wahr 2006, Landerer and Swenson 2012) at 1.0 degree resolution from January 2003 to December 2011 provided by the Jet Propulsion Laboratory. Monthly grids represent the mass deviation relative to the January 2004–December 2009 baseline and are implemented here as a proxy for water availability to vegetation. Four missing months of data were filled by taking the mean of the previous and subsequent months.

#### 3.2. AMSR-E vegetation optical depth (VOD)

The Advanced Microwave Scanning Radiometer—EOS (AMSR-E) is a microwave radiometer deployed on the polar-orbiting Aqua satellite. The VOD parameter derived from AMSR-E brightness temperatures, defines the frequency dependent extinction of land surface microwave emissions by the intervening vegetation layer (Jackson and Schmugge 1991, Van de Griend and Wigneron 2004, Jones and Kimball 2012). VOD is sensitive to changes in canopy biomass and water content, including both photosynthetic and woody elements (hereafter referred to as canopy biomass), and has been used to track both Amazon (Jones *et al* 2011) and African (Guan *et al* 2012) forest phenology. The VOD retrieval algorithm minimizes the potential influence of atmosphere precipitable water vapor, temperature, surface water inundation and soil moisture effects, providing near-daily global observations posted to a 25 km resolution global EASE grid projection (Jones *et al* 2011, Jones and Kimball 2012). For this application, the 10.7 GHz, descending orbit (UTC 1:30 A.M. equatorial crossings) VOD record from January 2003 to September 2011 was composited to a monthly mean time series consistent with the GRACE TWS record.

#### 3.3. Moderate resolution imaging spectroradiometer (MODIS) leaf area index (LAI) and EVI

The (MODIS) MOD15A2 8-day L4 Collection five LAI and an EVI (Huete *et al* 2002) derived from MODIS multiangle implementation of atmospheric correction (MAIAC) data (Lyapustin *et al* 2011a, 2011b, 2012) are used to track canopy leaf area and greenness, respectively, from January 2003 to December 2011 at 1 km resolution. The LAI product was

spatially resampled to match the VOD 25 km EASE grid format by taking the mean of all highest quality LAI pixels with pixel centers in the spatial extent of each 25 km pixel. The 8-day LAI record was then temporally resampled to monthly means.

#### 3.4. Clouds and the Earth's Radiant Energy System (CERES) photosynthetically active radiation

Gridded monthly 1.0 degree resolution diffuse and direct PAR data (CERES\_SYN1deg\_Ed3A) was used from the Clouds and the Earth's Radiant Energy System (CERES) (Wielicki *et al* 1996) record from January 2003 to December 2011. Total PAR was calculated as the sum of direct and diffuse PAR.

#### 3.5. Tropical Rainfall Monitoring Mission (TRMM) precipitation

TRMM 3B43 version seven Accumulated Rain monthly (cm/month) gridded data at 0.25 degree resolution from January 1998 to December 2011 was acquired from the Goddard Earth Sciences Data and Information Services Center. The pixel-wise number of months per year with less than 100 mm precipitation (dry months) were calculated and summarized by ecoregion (figure 1). Pearson product-moment cross-correlations between TRMM precipitation and GRACE TWS were calculated to examine the temporal offset between precipitation inputs and water availability.

#### 3.6. Terrestrial ecoregions

We used the World Wildlife Fund (WWF) Terrestrial Ecoregions of the World data set (Olson *et al* 2001) to distinguish ecoregion level changes in canopy seasonality. The WWF data contains 867 global ecoregions, each representing distinct assemblages of natural communities sharing a large majority of species, dynamics and environmental conditions. Nine terrestrial ecoregions spanning the west-to-east regional moisture gradient encompassing southern equatorial Amazon evergreen broadleaf forest were used in the analysis (figure 1). Monthly ecoregion means of the remotely sensed datasets were used to calculate monthly climatology and as inputs to a 4-parameter sinusoidal model (detailed in section 3.8) for estimating ecoregion scale phase shift differences between water availability (TWS), vegetation canopy biomass (VOD) and canopy leaf area (LAI) phenology.

#### 3.7. Plot level data and tower GEP, Pc

An extensive literature review located vegetation phenology field data within the ecoregions and general period of this study. Site specific field measurements within intact forests and without experimental manipulation (table S1) were found in two ecoregions (Tapajos–Xinghu, Xinghu–Tocantins–Araguaia). Although the temporal span of the field data was incomplete relative to the remote sensing record, with some data collected in prior years (1999–2002), these data constituted the only publicly available field observation record. Tower flux data of aggregated monthly GEP and Pc (table S1)

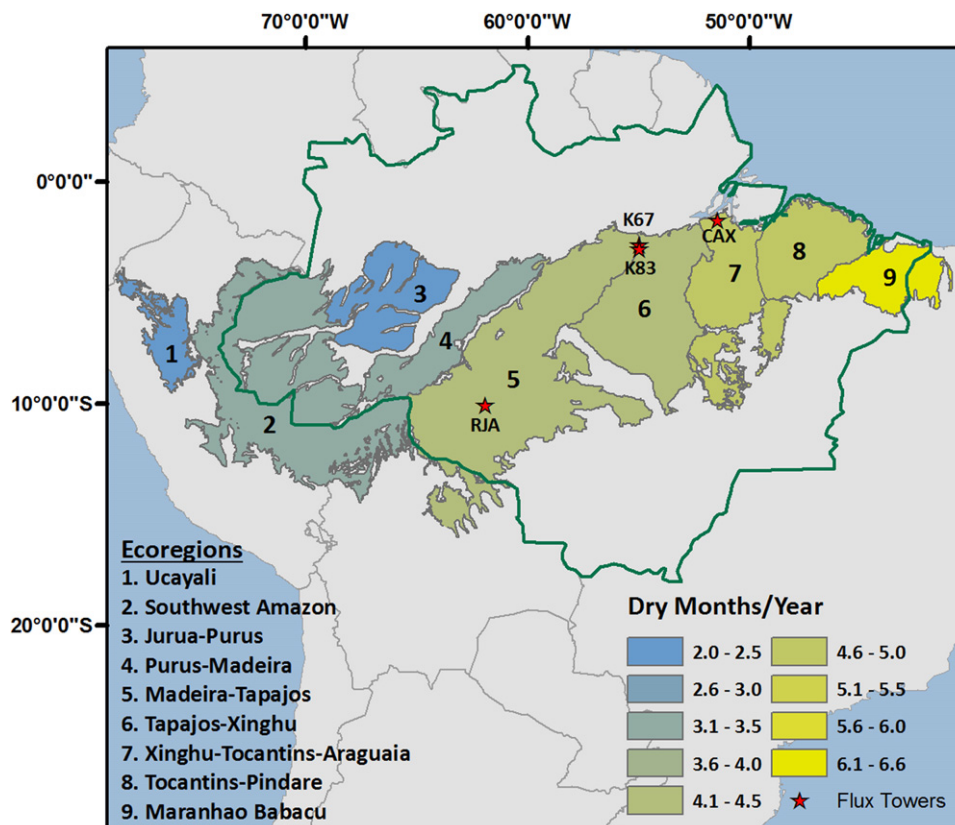


**Figure 1.** Amazon study domain showing southern equatorial ecoregions (Olson *et al* 2001) with the mean number of dry months (<100 mm) per year calculated from TRMM 3B43 version 7 Accumulated Rainfall at 0.25 degree resolution from 1998 to 2011. Flux tower locations used in this study are shown; Reserve Jaru (RJA), Tapajos K67 (K67), Tapajos K83 (K83) and Caxiuna (CAX) (table S1). The green border denotes the legal Amazon boundary in Brazil.

from the Large-Scale Biosphere–Atmosphere (LBA) Experiment in Amazonia was acquired from the LBA flux tower integrated database (Restrepo-Coupe *et al* 2013). The GEP data was calculated as the difference between day and night tower estimates of net ecosystem exchange of CO<sub>2</sub> (NEE), assuming no temperature effect on ecosystem respiration as no within-month correlation was observed between nighttime NEE and nighttime temperature at any sites studied. Pc (Pc not constrained by light) was calculated as GEP for a fixed range of PAR (725 < PAR < 925 μmol CO<sub>2</sub> m<sup>-2</sup> s<sup>-1</sup>). In this study, monthly GEP and Pc climatologies were calculated at four sites (RJA, K67, K83, CAX) within three ecoregions (figure 1). The field and flux tower observations are not implemented in the formal analysis, but are presented for comparison and interpretation of the satellite record.

### 3.8. Sinusoidal model fits to estimate ecoregion climatology

Monthly climatologies were calculated over the 2003–2011 record for TWS, VOD, LAI, EVI, and both total and direct PAR by ecoregion. We also implemented a 4-parameter sinusoidal fit (1) to the full TWS, VOD and LAI data records,

$$y_t = y_0 + a \sin\left(\frac{2\pi x}{b} + c\right), \quad (1)$$

where  $y_t$  is the fitted monthly climatology value,  $y_0$  is the

mean value,  $a$  is the amplitude of the sinusoidal curve,  $x$  is the monthly increment,  $b$  is the frequency, and  $c$  is the phase shift. Although this method gives a generalized monthly climatology interpretation, it provides a phase shift parameter ( $c$ ) quantifying the temporal offset between the three data sets within each ecoregion. The temporal offset in months was calculated as the phase shift difference divided by  $2\pi/b$ ;  $b$  in all cases was equivalent to 12 months (table S3), confirming a yearly cycle. Model results, specifically the temporal offset between the three data sets, was confirmed by a more robust pairwise bispectral analysis (see appendix 1 of supplementary information).

## 4. Results

### 4.1. Seasonality of Amazon forests

The satellite observations, when examined together over ecoregions and supported by available field and flux tower data, confirm that Amazon forest canopies exhibit seasonality (figure 2). The observed TWS seasonality is consistent with basin-wide model and field measurement based observations of PAW (Asner *et al* 2004, Brando *et al* 2010) and soil moisture (Fisher *et al* 2007). The observed VOD seasonality is synchronous with woody biomass increment growth

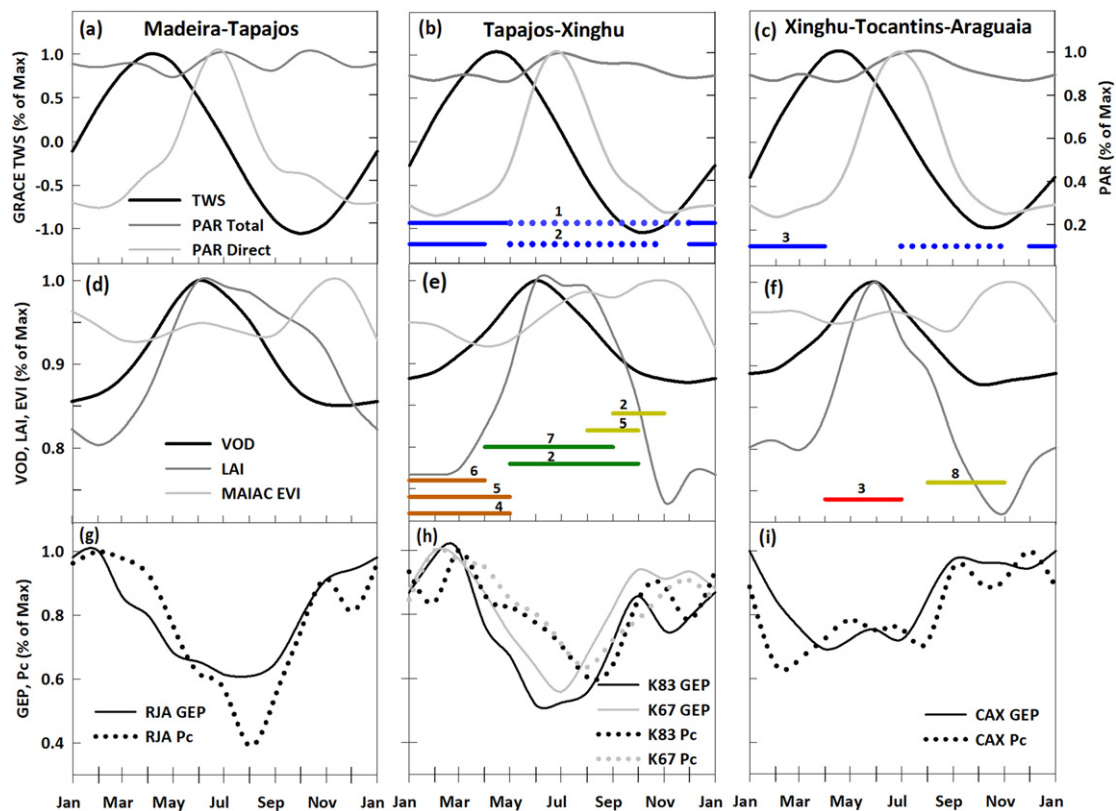


**Figure 2.** Monthly climatologies (plotted as the percentage of maximum) of satellite observations for Madeira–Tapajós (a), (d), (g), Tapajós–Xinghu (b), (e), (h) and Xinghu–Tocantins–Araguaia (c), (f), (i) ecoregions; satellite observations include TWS and direct and total PAR (a)–(c); VOD, LAI and MAIAC EVI (d)–(f). GEP and Pc from four flux tower sites are also presented (g)–(i), including Reserve Jaru (RJA), Tapajós K67 (K67), Tapajós K83 (K83) and Caxiuana (CAX) sites. Horizontal lines represent interpretations (i.e. examination of plots if specific data was not provided) of reported field data within ecoregions, including increasing (blue-solid) and decreasing (blue-dotted) PAW (1—Asner *et al* 2004, 2—Brando *et al* 2010) and soil water content (3—Fisher *et al* 2007); increasing woody growth (brown) (6—Saleska *et al* 2003, 4—Goulden and Miller 2004, 5—Rice *et al* 2004); increasing leaf flush (green) (7—Doughty and Goulden 2008, 2—Brando *et al* 2010); peaks in leaf litterfall rates (yellow) (5—Rice *et al* 2004, 8—Barlow *et al* 2007, 2—Brando *et al* 2010), and increasing sap flow (red) (3—Fisher *et al* 2007).

(Saleska *et al* 2003, Goulden and Miller 2004, Rice *et al* 2004) and sap flow (Fisher *et al* 2007) from available field measurements. Observed LAI and VOD seasonality is well aligned with field-level leaf production increases and peaks in litterfall rates (Rice *et al* 2004, Barlow *et al* 2007, Doughty and Goulden 2008, Brando *et al* 2010), while peaks in MAIAC EVI, a well-established proxy for photosynthetic C fixation, are temporally aligned with Pc and GEP from regional flux tower observations.

#### 4.2. Dry, wet seasons and water availability in the Amazon

Pearson product-moment cross-correlations between TRMM precipitation and GRACE TWS at the ecoregion scale were greatest at a two months lag ( $0.78 < R < 0.91$ ) for seven ecoregions and a three months lag ( $0.89 < R < 0.91$ ) for two ecoregions (table S2). These results confirm a reported two months lag between precipitation inputs and TWS across eight Amazon sub-basins (Frappart *et al* 2013) and a 2–3 months lag between peak precipitation and river level and stream flow observations (Marengo *et al* 2008). Thus,

seasonal minima in plant-available moisture indicated from bulk TWS changes occur months after the initial dry season (precipitation  $< 100$  mm/month) onset, which is also confirmed by estimates and measures of plant-available water at variable soil depths (Asner *et al* 2004, Fisher *et al* 2007, Brando *et al* 2010). Therefore, equating dry months to periods of minimum water availability represents an oversimplification of ecosystem water dynamics and neglects hydraulic transport processes and water residence times, which can be considerable in the Amazon basin.

#### 4.3. Seasonal phase shifts in TWS, VOD, and LAI

The resulting coefficients and statistics from the sinusoidal model fits are displayed in (table S3). The sinusoidal model ecoregion climatology of TWS, VOD, and LAI each displayed seasonal phase shifts along the west-to-east moisture gradient (figure 3). GRACE TWS displayed a two months shift in seasonal peak over the Amazon, ranging from March in the west to May in the east. VOD displayed a one month shift, peaking in June in the west and July in the east; LAI

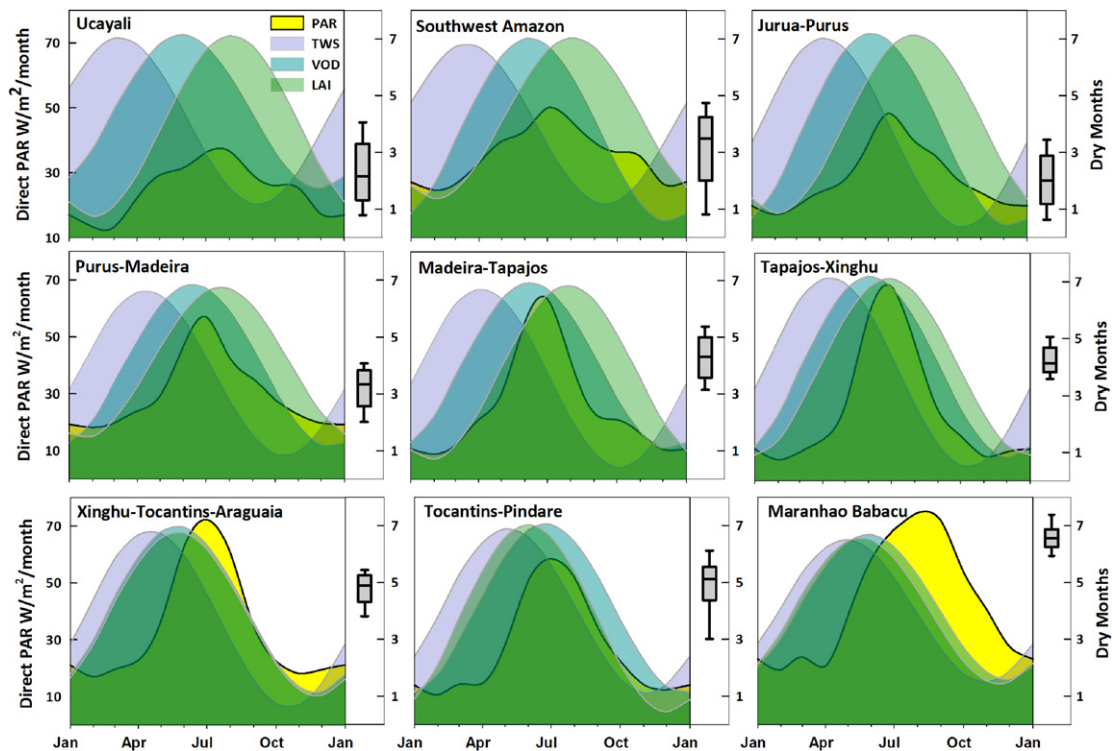


**Figure 3.** Sinusoidal model climatology for TWS, VOD and LAI; direct PAR monthly climatology and statistics (box plots) of dry months per year by ecoregion. TWS, VOD and LAI, are plotted as anomalies from the long-term means (mean value ( $y_0$ )) subtracted from fitted values ( $y_t$ )), and the y-axis (not shown) for TWS, VOD, and LAI are relatively scaled for visual interpretation of phase shifts. Box plots display median, 25th and 75th percentiles, and 10th and 90th percentiles. Ecoregion plots are ordered from west (top left) to east (bottom right).

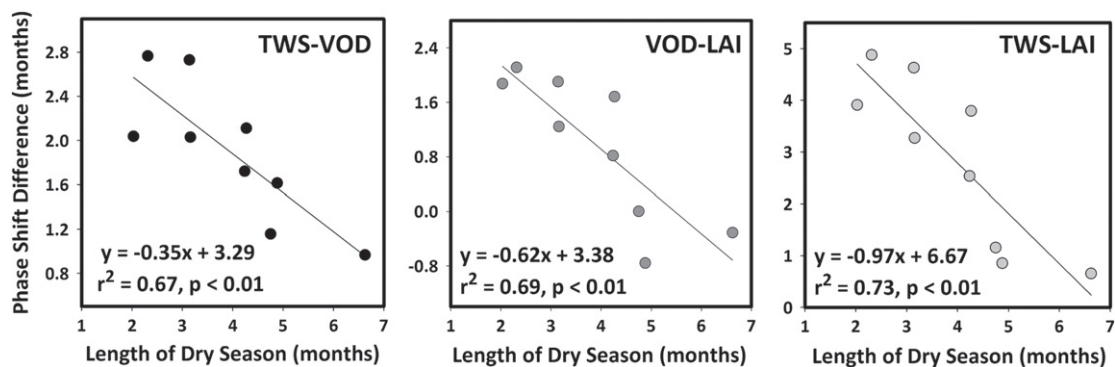


**Figure 4.** Least-squares linear regression relationships between mean dry season length from TRMM and associated phase shift differences (months) for TWS and VOD, VOD and LAI, and TWS and LAI by ecoregion.

displayed the greatest shift of 2.5 months, with western peaks occurring in August and eastern peaks in mid-May.

The ecoregion phase shift difference between the three datasets decreased with increasing dry season across the west-to-east moisture gradient (figure 3). VOD seasonality lagged TWS by a maximum of 2.8 months to a minimum of 1 month. LAI seasonality lagged TWS by 4.9–0.7 months. LAI seasonality lagged VOD for 5 of 9 ecoregions by 2.1–0.8 months, was equivalent (no lag) for one ecoregion, and preceded VOD by 0.3–0.8 months for the remaining two ecoregions. The phase shift differences all displayed significant negative linear relationships ( $0.67 < r^2 < 0.73$ ;  $p < 0.01$ ) with dry season length by ecoregion (figure 4), where VOD, LAI

and TWS seasonal patterns are more synchronous for ecoregions with longer dry seasons.

#### 4.4. Estimates of canopy phenology adaptation to light and water availability

The linear relationship between dry season length and the phase shift difference between VOD and LAI (figure 4) was used to estimate relative canopy phenology adaptations to light and water availability. The mean number of dry months per pixel from the 0.25 degree TRMM data was input to the linear model to estimate expected pixel-wise phase shifts between VOD and LAI. The resulting phase shifts provide a

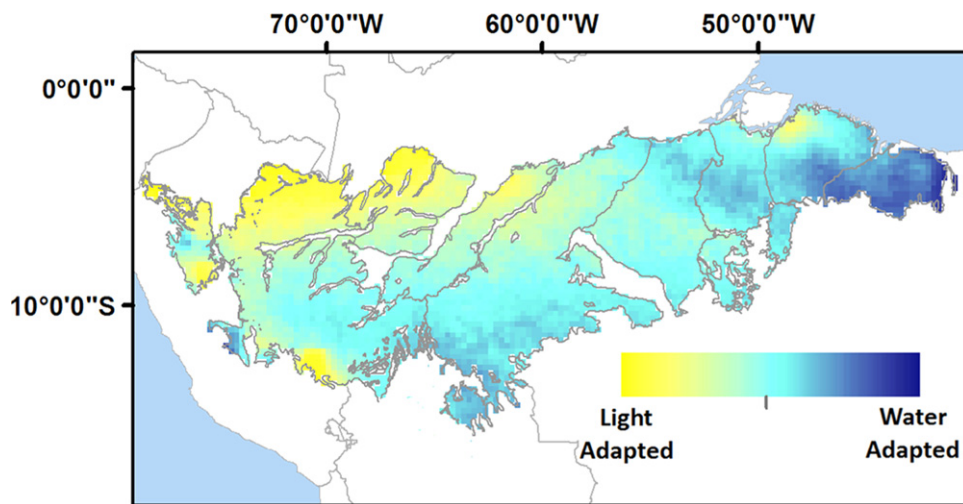


**Figure 5.** Pixel-wise (0.25 degree) relative canopy phenology adaptation to light or water availability based on the linear relationship between the mean number of dry months per pixel from TRMM precipitation, and the seasonal phase shift between VOD and LAI across ecoregions. Yellow (blue) pixels denote areas where canopy water uptake and timing of canopy development and growth have adapted predominantly to light (water) availability, with dry season generally increasing from west to east, respectively.

proxy for the degree to which the timing of canopy growth and development has adapted primarily to light (maximal phase shift) or water (minimal phase shift) availability (figure 5).

## 5. Discussion

### 5.1. The transition from light-adapted to water-adapted regions

The southern equatorial Amazon ecoregions represent a west-to-east transition from predominantly light-adapted to water-adapted canopy phenology (figure 5). The observed canopy behavior supports current theories that net leaf flush is responsive to solar irradiance, but also demonstrates an adaptive response to limit drought susceptibility, even in relatively precipitation rich regions, for efficient temporal allocation of resources for wood or leaf growth. In more light-adapted western ecoregions (figure 3, row 1), available water (TWS) reaches maximum levels during seasonal lows in direct PAR and allocation of resources to non-photosynthetic canopy elements is prioritized, displayed as a rise in VOD and confirmed by field measures of wet season woody growth (Saleska *et al* 2003, Goulden and Miller 2004, Rice *et al* 2004). The VOD rise is also consistent with canopy water content increases required for cellular expansion and new leaf formation (Pantin *et al* 2012). Increases in LAI (i.e. the net flush of new leaves) coincides with seasonal increases in direct PAR, representing a shift in resource allocation from woody to leaf growth. Decreasing LAI (i.e. peaks in net leaf senescence and abscission) is then observed as available water (TWS) reaches seasonal lows and canopy biomass (VOD) declines. Canopy greenness (EVI) and productivity (Pc and GEP) then rise as the new cohort of leaves reach photosynthetic maturity, which has been reported to occur up to approximately 40 days following full leaf expansion for tropical species (Niinemets *et al* 2012).

As dry season length increases, a general transition from light-adapted to water-adapted canopy phenology becomes apparent (figure 5). For longer dry seasons (figure 3, row 2), seasonal net leaf flush (LAI) becomes more synchronous with canopy biomass (VOD) increases, yet maintains comparable seasonality with direct PAR and remains somewhat decoupled from water availability (TWS). As dry season increases further (figure 3, row 3) and water becomes more limiting, net leaf flush (LAI) and canopy biomass (VOD) become tightly coupled to water availability (TWS) and begin to lag direct PAR seasonality, characteristics attributable to drought-tolerant systems where water deficits, increasing temperatures and inhibitory atmosphere vapor pressure deficits coincide with seasonal peaks in direct solar irradiance.

### 5.2. Solar irradiance seasonality

Top-of-atmosphere irradiance seasonality varies with latitude and solar azimuth angle, but total PAR seasonality at the ecoregion scale displays relatively small seasonal increases, on the order of 11–18% (figure 2), due to cloud cover seasonality. The low PAR seasonality perhaps counters the theory that leaf growth is responsive to increases in irradiance, which is not obvious when examining the climatology of total PAR and LAI (figure 2). However, the amount of quanta, which ultimately drives photosynthesis, can vary with no change in total PAR. Diffuse solar irradiance, enriched by blue quanta with higher energy, contains less quanta than direct irradiance with a more uniform spectral distribution (Valladares *et al* 2012); the photosynthetically active photon-flux density (PPFD) of diffuse irradiance will be lower than direct irradiance at equal PAR. The endogenous response that drives synchronous net leaf flush with increases in direct PAR in light-adapted systems (figure 3) may be responsive to increases in PPFD associated with the transition from diffuse-dominated to direct-dominated PAR.



### 5.3. Implications for drought tolerance

In ecoregions that experience short dry seasons, net leaf flush is synchronized with direct PAR resulting in canopy leaf area peaks during periods of lowest water availability. If water availability were to decline below critical thresholds following leaf flush (i.e. drought years) would ecoregions that exhibit asynchrony between net leaf flush and water availability display greater detrimental canopy effects (e.g. lack of available water to support a new cohort of leaves) than ecoregions that exhibit net leaf flush synchronous with water availability? A study of the 2005 and 2010 Amazon droughts (Xu *et al* 2011), which spanned approximately 2.5 and 3.2 million km<sup>2</sup>, respectively (Lewis *et al* 2011, Xu *et al* 2011), and were among the driest years of record based on river observations dating to 1902 (Xu *et al* 2011), provides context for addressing this question. Of the vegetated area that experienced significant declines in precipitation in 2010, 51% displayed significant declines in satellite observed greenness (NDVI) during July, August, September (JAS) and October, November, December (OND) composite periods. The areas affected in 2010 were located in all ecoregions used in this study, indicating that even eastern ecoregions with drought tolerant phenology (net leaf flush synchronous with available water) could not withstand the extreme water limitations. In contrast, of the vegetated area that experienced significant declines in precipitation in 2005, 14% displayed significant declines in greenness during the JAS composite period. However, during the OND composite period western ecoregions displayed an increase in area of significant greenness decline while eastern ecoregions displayed some recovery to normal greenness. Although further research is needed, western ecoregions displaying light-adapted canopy phenology (net leaf flush asynchronous with water availability) may be more sensitive to detrimental drought effects.

### 5.4. Modeling applications

Seasonal phase differences between canopy phenology and light and water availability indicators documented in this study may improve understanding, and parameterizations and representations, of canopy processes in regional carbon and climate models. Regions that display light-adapted canopy phenology can be weighted for greater sensitivity to solar irradiance seasonality, while regions displaying water-adapted canopy phenology can be driven primarily by water availability and estimates of rooting depth (Nepstad *et al* 1994) and hydraulic redistribution (Da and Goulden 2004). Investigating these phase differences at moderate spatial scales may allow for a classification scheme, whereby the driving factor of canopy phenology (whether it be water or light, or a combination thereof) is based on the phase difference between satellite derived water availability, canopy biomass, and leaf flush, as displayed in figure 5. Such an effort would allow for more specific modeling of canopy phenology across contiguous tropical forests.

## 6. Conclusion

This study provides evidence from six independent satellite data records, and available ground observations and reported field studies, that southern equatorial Amazon forests have a distinctive canopy phenology that is responsive to seasonal changes in both water availability and solar radiation. Our results support the hypothesis that net leaf flush in tropical forests is responsive to solar irradiance seasonality, but is also responsive to variations in dry season length and associated water availability supporting vegetation growth. The timing of water availability, canopy biomass growth and net leaf flush are asynchronous in regions with short dry seasons and become more synchronous across a west-to-east longitudinal moisture gradient of increasing dry season length. These results have important implications for modeling efforts by providing insight into the abiotic cues that influence tropical forest phenology and the temporal allocation of resources to woody versus foliar growth. They also provide a means to estimate region specific sensitivity to drought and anticipated drying under projected future climate conditions.

## Acknowledgments

We thank the flux tower Principal Investigators, S Wofsy, V Kirckhoff, Goulden, da Rocha, M Waterloo, A Manzi, and L Sa of the Large Scale Biosphere–Atmosphere Experiment in Amazonia (LBA) for making their data freely available and Alexei Lyapustin for creating the MODIS MAIAC data. We also thank Saleska, da Rocha, Restrepo-Coupe, Huete, A Nobre, P Artaxo, and Y Shimabukuro for creating the publicly available LBA flux tower integrated database, Dr Cory Cleveland for his valuable input, and the anonymous reviewers for their valuable input and suggestions which improved this manuscript. The GRACE land data (available at <http://grace.jpl.nasa.gov>) processing algorithms were provided by Sean Swenson, and supported by the NASA MEASUREs program. This work was performed at the University of Montana, and the Ames Research Center with funding provided by the NASA Science of Terra and Aqua program (NNX11AD46G).

## References

- Asner G P, Nepstad D, Cardinot G and Ray D 2004 Drought stress and carbon uptake in an Amazon forest measured with spaceborne imaging spectroscopy *Proc. Natl Acad. Sci. USA* **101** 6039–44
- Baker I T, Prihodko L, Denning A S, Goulden M, Miller S and da Rocha H R 2008 Seasonal drought stress in the Amazon: reconciling models and observations *J. Geophys. Res.* **113** G00B01
- Barlow J, Gardner T A, Ferreira L V. and Peres C A 2007 Litter fall and decomposition in primary, secondary and plantation forests in the Brazilian Amazon *For. Ecol. Manag.* **247** 91–7

- Brando P M, Goetz S J, Baccini A, Nepstad D C, Beck P S and Christman M C 2010 Seasonal and interannual variability of climate and vegetation indices across the Amazon *Proc. Natl Acad. Sci. USA* **107** 14685–90
- Chen J L, Wilson C R and Tapley B D 2010 The 2009 exceptional Amazon flood and interannual terrestrial water storage change observed by GRACE *Water Resour. Res.* **46** W12526
- Christensen J H *et al* 2007 Regional climate projections *Climate Change 2007: The Physical Science Basis. Contribution of Working Group I to the Fourth Assessment Report of the Intergovernmental Panel on Climate Change* ed S Solomon *et al* (Cambridge: Cambridge University Press) ([www.ipcc.ch/pdf/assessment-report/ar4/wg1/ar4-wg1-chapter11.pdf](http://www.ipcc.ch/pdf/assessment-report/ar4/wg1/ar4-wg1-chapter11.pdf))
- Cox P M, Harris P P, Huntingford C, Betts R A, Collins M, Jones C D, Jupp T E, Marengo J A and Nobre C A 2008 Increasing risk of Amazonian drought due to decreasing aerosol pollution *Nature* **453** 212–5
- Cox P M, Pearson D, Booth B B, Friedlingstein P, Huntingford C, Jones C D and Luke C M 2013 Sensitivity of tropical carbon to climate change constrained by carbon dioxide variability *Nature* **494** 341–4
- Doughty C E and Goulden M L 2008 Seasonal patterns of tropical forest leaf area index and CO<sub>2</sub> exchange *J. Geophys. Res.* **113** 1–12
- Fisher R A, Williams M, da COSTA A L, Malhi Y, da COSTA R F, Almeida S and Meir P 2007 The response of an Eastern Amazonian rain forest to drought stress: results and modelling analyses from a throughfall exclusion experiment *Glob. Change Biol.* **13** 2361–78
- Frankenberg C, O'Dell C, Berry J, Guanter L, Joiner J, Köhler P, Pollock R and Taylor T E 2014 Prospects for chlorophyll fluorescence remote sensing from the orbiting carbon observatory-2 *Remote Sens. Environ.* **147** 1–12
- Frappart F, Ramillien G and Ronchail J 2013 Changes in terrestrial water storage versus rainfall and discharges in the Amazon basin *Int. J. Climatol.* **33** 3029–46
- Frolking S, Milliman T, Palace M, Wisser D, Lammers R and Fahnestock M 2011 Tropical forest backscatter anomaly evident in seawinds scatterometer morning overpass data during 2005 drought in Amazonia *Remote Sens. Environ.* **115** 897–907
- Goulden M and Miller S 2004 Diel and seasonal patterns of tropical forest CO<sub>2</sub> exchange *Ecol. Appl.* **14** 42–54
- Griend A A V D, Wigneron J and Member S 2004 On the measurement of microwave vegetation properties: some guidelines for a protocol *IEEE Trans. Geosci. Remote Sens.* **42** 2277–89
- Guan K, Wood E F and Caylor K K 2012 Multi-sensor derivation of regional vegetation fractional cover in Africa *Remote Sens. Environ.* **124** 653–65
- Huete A, Didan K, Miura T, Rodriguez E P, Gao X and Ferreira L G 2002 Overview of the radiometric and biophysical performance of the MODIS vegetation indices *Remote Sens. Environ.* **83** 195–213
- Jackson T J and Schmugge T J 1991 Vegetation effects on the microwave emission of soils *Remote Sens. Environ.* **36** 203–12
- Jones L A and Kimball J S 2012 *Daily Global Land Surface Parameters Derived from AMSR-E* (Boulder, CO: NASA DAAC at the National Snow and Ice Data Center) (<http://nsidc.org/data/nsidc-0451.html>)
- Jones M O, Jones L A, Kimball J S and McDonald K C 2011 Satellite passive microwave remote sensing for monitoring global land surface phenology *Remote Sens. Environ.* **115** 1102–14
- Kim Y, Knox R G, Longo M, Medvigy D, Hutryra L R, Pyle E H, Wofsy S C, Bras R L and Moorcroft P R 2012 Seasonal carbon dynamics and water fluxes in an Amazon rainforest *Glob. Change Biol.* **18** 1322–34
- Kim Y, Knox R G, Longo M, Medvigy D, Hutryra L R, Pyle E H, Wofsy S C, Bras R L and Moorcroft P R 2012 Seasonal carbon dynamics and water fluxes in an Amazon rainforest *Glob. Change Biol.* **18** 1322–34
- Landerer F W and Swenson S C 2012 Accuracy of scaled GRACE terrestrial water storage estimates *Water Resour. Res.* **48** 11W04531
- Lee J and Oliveira R 2005 Root functioning modifies seasonal climate *Proc. Natl Acad. Sci. USA* **102** 17576–81
- Lee J-E, Lintner B R, Boyce C K and Lawrence P J 2011 Land use change exacerbates tropical South American drought by sea surface temperature variability *Geophys. Res. Lett.* **38** L19706
- Lee J-E *et al* 2013 Forest productivity and water stress in Amazonia: observations from GOSAT chlorophyll fluorescence *Proc. R. Soc. B* **280** 20130171
- Lewis S L, Brando P M, Phillips O L, van der Heijden G M F and Nepstad D 2011 The 2010 Amazon drought *Science* **331** 554
- Li W, Fu R, Juárez R I N and Fernandes K 2008 Observed change of the standardized precipitation index, its potential cause and implications to future climate change in the Amazon region *Phil. Trans. R. Soc. B* **363** 1767–72
- Lyapustin A, Martonchik J, Wang Y, Laszlo I and Korkin S 2011a Multi-angle implementation of atmospheric correction (MAIAC):1. Radiative transfer basis and look-up tables *J. Geophys. Res.* **116** D03210
- Lyapustin A, Wang Y, Laszlo I, Kahn R, Korkin S, Remer L, Levy R and Reid J S 2011b Multi-angle implementation of atmospheric correction (MAIAC):2. Aerosol algorithm *J. Geophys. Res.* **116** D03211
- Lyapustin A, Wang Y, Laszlo I, Hilker T, Hall F, Sellers P, Tucker J and Korkin S 2012 Multi-angle implementation of atmospheric correction for MODIS (MAIAC):3. Atmospheric correction *Remote Sens. Environ.* **127** 385–93
- Malhi Y, Aragão L E O C, Galbraith D, Huntingford C, Fisher R, Zelazowski P, Sitch S, McSweeney C and Meir P 2009 Exploring the likelihood and mechanism of a climate-change-induced dieback of the Amazon rainforest *Proc. Natl Acad. Sci.* **106** 20610–5
- Marengo J A, Nobre C A, Tomasella J, Oyama M D, Sampaio de Oliveira G, de Oliveira R, Camargo H, Alves L M and Brown I F 2008 The drought of Amazonia in 2005 *J. Clim.* **21** 495–516
- Moorcroft P, Hurtt G and Pacala S 2001 A method for scaling vegetation dynamics: the ecosystem demography model (ED) *Ecol. Monogr.* **71** 557–85
- Morton D C, Nagol J, Carabajal C C, Rosette J, Palace M, Cook B D, Vermote E F, Harding D J and North P R J 2014 Amazon forests maintain consistent canopy structure and greenness during the dry season *Nature* **506** 221–4
- Myneni R B *et al* 2007 Large seasonal swings in leaf area of Amazon rainforests *Proc. Natl Acad. Sci. USA* **104** 4820–3
- Nepstad D C, de Carvalho C R, Davidson E A, Jipp P H, Lefebvre P A, Negreiros G H, da Silva E D, Stone T A, Trumbore S E and Vieira S 1994 The role of deep roots in the hydrological and carbon cycles of Amazonian forests and pastures *Nature* **372** 666–9
- Niinemets U, Garcia-Plazaola J I and Tosens T 2012 Photosynthesis during leaf development and ageing ed J Flexas *et al* *Terrestrial Photosynthesis in a Changing Environment. A Molecular, Physiological, and Ecological Approach* (Cambridge: Cambridge University Press) pp 353–72
- Olson D M *et al* 2001 Terrestrial ecoregions of the world: a new map of life on Earth *Bioscience* **51** 933
- Pantin F, Simonneau T and Muller B 2012 Coming of leaf age: control of growth by hydraulics and metabolics during leaf ontogeny *New Phytol.* **196** 349–66
- Parazoo N C *et al* 2013 Interpreting seasonal changes in the carbon balance of southern Amazonia using measurements of XCO<sub>2</sub>

- and chlorophyll fluorescence from GOSAT *Geophys. Res. Lett.* **40** 2829–33
- Phillips O L *et al* 2009 Drought sensitivity of the Amazon rainforest *Science* **323** 1344–7
- Restrepo-Coupe N *et al* 2013 What drives the seasonality of photosynthesis across the Amazon basin? A cross-site analysis of eddy flux tower measurements from the Brasil flux network *Agric. For. Meteorol.* **182–3** 128–44
- Rice A, Pyle E and Saleska S 2004 Carbon balance and vegetation dynamics in an old-growth Amazonian forest *Ecol. Appl.* **14** S55–71
- Rocha H D and Goulden M 2004 Seasonality of water and heat fluxes over a tropical forest in eastern Amazonia *Ecol. Appl.* **14** 22–32
- Rowland L, Hill T C, Stahl C, Siebicke L, Burban B, Zaragoza-Castells J, Ponton S, Bonal D, Meir P and Williams M 2014 Evidence for strong seasonality in the carbon storage and carbon use efficiency of an Amazonian forest *Glob. Change Biol.* **20** 979–91
- Saatchi S S *et al* 2011 Benchmark map of forest carbon stocks in tropical regions across three continents *Proc. Natl Acad. Sci. USA* **108** 9899–904
- Salazar L F, Nobre C A and Oyama M D 2007 Climate change consequences on the biome distribution in tropical South America *Geophys. Res. Lett.* **34** L09703
- Saleska S R *et al* 2003 Carbon in Amazon forests: unexpected seasonal fluxes and disturbance-induced losses *Science* **302** 1554–7
- Samanta A, Knyazikhin Y, Xu L, Dickinson R E, Fu R, Costa M H, Saatchi S S, Nemani R R and Myneni R B 2012 Seasonal changes in leaf area of Amazon forests from leaf flushing and abscission *J. Geophys. Res.* **117** 1–13
- Schaik C V, Terborgh J and Wright S 1993 The phenology of tropical forests: adaptive significance and consequences for primary consumers *Annu. Rev. Ecol.* **24** 353–77
- Silva F B, Shimabukuro Y E, Aragão L E O C, Anderson L O, Pereira G, Cardozo F and Arai E 2013 Corrigendum: large-scale heterogeneity of Amazonian phenology revealed from 26 years long AVHRR/NDVI time-series *Environ. Res. Lett.* **8** 029502
- Swenson S C and Wahr J 2006 Post-processing removal of correlated errors in GRACE data *Geophys. Res. Lett.* **33** L08402
- Thomas A and Reager J 2014 A GRACE-based water storage deficit approach for hydrological drought characterization *Geophys. Res. Lett.* **41** 1537–45
- Valladares F, García Plazaola J I, Morales F and Niinemets U 2012 Photosynthetic responses to radiation *Terrestrial Photosynthesis in a Changing Environment. A Molecular, Physiological, and Ecological Approach* ed J Flexas *et al* (Cambridge: Cambridge University Press) pp 239–56
- Van De Griend A A and Wigneron J 2004 On the measurement of microwave vegetation properties: some guidelines for a protocol *IEEE Trans. Geosci. Remote Sens.* **42** 2277–89
- Wielicki B, Barkstrom B, Harrison E, Lee R III, Smith G and Cooper J 1996 Clouds and the Earth's Radiant Energy System (CERES): an earth observing system experiment *Bull. Am. Meteorol. Soc.* **77** 853–68
- Wright S J 1996 *Phenological Responses to Seasonality in Tropical Forest Plants, Tropical Forest Plant Ecophysiology SE—15* ed S Mulkey *et al* (Berlin: Springer) pp 440–60
- Wright S J and Schaik C V 1994 Light and the phenology of tropical trees *Am. Nat.* **143** 192–9
- Xiao X, Zhang Q, Saleska S, Hutyrá L, De Camargo P, Wofsy S, Frohking S, Boles S, Keller M and Moore B 2005 Satellite-based modeling of gross primary production in a seasonally moist tropical evergreen forest *Remote Sens. Environ.* **94** 105–22
- Xu L, Samanta A, Costa M H, Ganguly S, Nemani R R and Myneni R B 2011 Widespread decline in greenness of Amazonian vegetation due to the 2010 drought *Geophys. Res. Lett.* **38** 2–5